Int. J. Electrochem. Sci., 16 **(2021)** Article ID: 210734, doi: 10.20964/2021.07.64

International Journal of
ELECTROCHEMICAL
SCIENCE
www.electrochemsci.org

Short Communication

Preparation of Algae Extract as Green Corrosion Inhibitor for Q235 Steel in Chloride Ion Solutions

Dengdeng Zheng[*] *and Guojie Wang*

School of Engineering, Fujian Jiangxia University, Fuzhou, Fujian 350108, China
[*]E-mail: ddzheng@vtcuni.com

Received: 19 March 2021 / *Accepted:* 9 May 2021 / *Published:* 31 May 2021

Adding corrosion inhibitor in corrosive medium is one of the effective methods to solve the corrosion of steel materials. In recent years, corrosion inhibitors of plant extracts have become a research hotspot. However, there are few studies on the corrosion inhibitors of algae extract. It is of great theoretical and practical application value to study the corrosion inhibition performance of algae extract. In this work, with algae as the raw material of corrosion inhibitor, the effects of different concentrations of algae extract on the corrosion behavior of Q235 steel were studied by means of self-corrosion potential time curve and polarization curve. The effective corrosion inhibition components of algae extracts were preliminarily determined by Fourier transform infrared spectroscopy. The corrosion morphology of Q235 steel in hydrochloric acid solution with or without corrosion inhibitor was characterized by scanning electron microscope.

Keywords: Algae extract; Q235 steel; Corrosion inhibitor; Fourier transform infrared spectroscopy; Electrochemical characterization

1. INTRODUCTION

Corrosion inhibitor is a chemical substance or a mixture of several chemical substances existing in the environment in appropriate concentration and form to slow down the corrosion. In general, corrosion inhibitor is a kind of substance that can effectively prevent metal corrosion without affecting the physical and mechanical properties of metal. Reasonable use of corrosion inhibitors can effectively prevent or significantly slow down the corrosion process of metals and their alloys in the environment [1–3]. The effective use of corrosion inhibitor in industrial production and life can greatly reduce the economic loss caused by corrosion. Therefore, the technology of corrosion inhibitor has drawn more and more attention [4,5]. The inhibitor has no fixed structure or composition. The selection mainly relates to the application environment. In addition, the type of corrosion inhibitor is only a single substance, and

it can also produce synergistic effect with other substances. This can significantly enhance the inhibition effect [6,7].

Corrosion inhibitor can prevent metal from corrosion by forming a layer of film on the surface of metal, so as to inhibit the corrosion medium in the environment from directly contacting metal[8–10]. According to the current research progress, it is difficult for a single component to produce ideal corrosion inhibition effect. Therefore, the corrosion inhibitors used in the actual production and life are mainly composed of a variety of components [11–13] that can achieve better inhibition effect than single one through synergistic effect [14–16].

Corrosion inhibitors were first extracted from plants, and then are made from other raw materials with the economic development. In the 21st century, the sustainable development of social ecology is threatened as a result of increasingly serious environmental pollution. With the development of society, it is urgent to develop new green corrosion inhibitors with low toxicity and easy degradation. The corrosion inhibitors extracted from natural plants have many advantages, such as low toxicity, low residue, easy degradation, simple process and low economic cost [17–21]. Sathyanathan et al. [22] confirmed that castor leaf extract can inhibit the corrosion of carbon steel in acidic medium. Gunasekaran et al. [23] investigated the corrosion inhibition effect of *Zanthoxylum bungeanum* extract on low-carbon steel in phosphoric acid solution and that of water coconut (Palmaceae) leaf extract on low-carbon steel in hydrochloric acid medium. Plants, flowers, and fruits have also been proved to have good corrosion inhibition effect. Parikh et al. [24] verified that *Momordica charantia* has corrosion inhibition effect on low-carbon steel in hydrochloric acid medium. Sethuraman et al. [25] studied the extract of *Datura stramonium* as a corrosion inhibitor for medium and low-carbon steel in hydrochloric acid medium. The work mainly focused on the inhibition effect of terrestrial plant extracts, not on aquatic plants. Mansou et al. [26] studied a coating containing green algae, which can inhibit the corrosion of carbon steel in seawater. Algae is the largest plant group in marine life, which is widely distributed [27–31]. They have low requirements for environmental conditions and show strong reproductive capacity. Marine algae not only contain a variety of amino acids, vitamins and other nutrients, but also contain a variety of rare bioactive and chemical active ingredients of terrestrial plants [32,33]. It is of great potential to study the components of marine plant extracts and develop new corrosion inhibitors.

By using the electrochemical method, the open circuit potential, electrochemical impedance spectroscopy and dynamic polarization curve were analyzed to study the corrosion inhibition effect of materials. Among them, electrochemical impedance spectroscopy was mainly used to analyze the mechanism of corrosion process, which can well simulate the electrode reaction process [34–36]. The corrosion potential, corrosion current density, Tafel cathode slope and anode slope of the metal can be obtained by potentiodynamic polarization curve test, and then the corrosion inhibition performance and mechanism of the inhibitor can be analyzed [37–49]. In this work, the effect of algae extract on the corrosion behavior of Q235 steel was investigated by the electrochemical method, Fourier transform infrared spectroscopy (FTIR) and scanning electron microscopy (SEM). Firstly, the corrosion behavior and inhibition efficiency of algae extract with different concentrations on Q235 steel in hydrochloric acid pickling solution were investigated by the electrochemical method. Then, the adsorption behavior of inhibitor molecules on Q235 steel surface was studied by using the physical and chemical theory, and the corresponding thermodynamic and kinetic parameters were calculated. Then, the effective corrosion

inhibition components of algae extracts were preliminarily determined by FTIR. Finally, the corrosion morphology of Q235 steel after immersion in hydrochloric acid pickling solution with or without corrosion inhibitor was characterized by SEM.

2. MATERIALS AND METHODS

Preparation of algae extract: Algae purchased (*Laminaria Japonica*) was washed with tap water. Deionized water was added to the algae, pressed into thick shape with a juicer. Then it was put on a magnetic stirrer and was stirred evenly for 2 hours. After filtration, the filtrate was dried in an oven at 30 ℃ to obtain the powder extract.

Weight loss experiment: The Q235 specimens were polished with 400 #, 800 #, 1000 # sandpaper, then degreased with anhydrous ethanol and acetone, weighed and measured with vernier calipers. The three specimens were placed in the solution with different corrosion inhibitor concentrations, reaction time, temperature and acid concentrations. The corrosion rate V and corrosion inhibition efficiency η were calculated using following equations.

$$V = \frac{m_0 - m}{St}$$

Where V is the corrosion rate, m_0 and m are the mass of the block before and after corrosion, S is the surface area of the steel block, t is the immersion time.

$$\eta = \frac{V_0 - V}{V_0}$$

Where V_0 and V are the corrosion rates of Q235 specimens in hydrochloric acid solutions without and with corrosion inhibitors, respectively

Electrochemical test: With 1 M HCl solution as the corrosion medium, the electrochemical test was carried out using standard three electrode system. The working electrode, reference electrode and auxiliary electrode were Q235 steel, saturated calomel electrode and platinum plate electrode, respectively. Q235 steel electrode was coated with epoxy resin except 1 cm^2 active surface. The working electrodes were polished with 400#, 800# and 1000# sandpaper. Then, it was washed with ethanol and acetone and inserted into the system for test. Firstly, the open circuit potential (OCP) curve with time was measured. EIS (frequency range: 0.01-100 kHz, signal amplitude: 10 mV) and potentiodynamic polarization curve (scanning range: E_{ocp} -500 mV ~ E_{ocp} +500 mV, scanning rate: 0.1 mV/s) were measured.

Characterization: FTIR (TENSOR27) was used to analyze the surface functional group of the algae extract; and SEM (TESCAN VEGAII LMU) was used to observe the morphology change before and after corrosion.

3. RESULTS AND DISCUSSION

Weight loss experiment was conducted first for testing the Q235 in 1M HCl with different concentrations of algae extract. Figure 1A shows the corrosion rate of algae extract with different

concentrations on Q235 steel in 1 M HCl at room temperature. When the concentration of algae extract was less than 100 mg/L, the corrosion rate of Q235 steel decreased significantly with the increase of algae extract concentration. When the concentration of the extract was more than 100 mg/L, the corrosion rate changed little. Therefore, when testing the effect of extract concentrations on corrosion rate at other temperature, the initial concentration was 100 mg/L. The inset of Figure 1 A is a digital photo of the algae extract used.

Figure 1B shows the corrosion rate of Q235 steel in 1 M HCL at 20 ~ 60 ℃. The results showed that the corrosion rate of Q235 steel decreased significantly with the addition of algae extract in the test temperature range. At the same temperature, the corrosion rate of carbon steel gradually decreased with the increase of extract concentration. When the concentration of the extract reached 200 mg/L, the corrosion rate changed little with the increase of the concentration of the extract. The results showed that the corrosion rate of Q235 steel increased with the increase of temperature when the same concentration of extract was added. With the increase of temperature, the movement speed of particles accelerated, leading to the aggravation of corrosion reaction [50,51]. The corrosion rate of Q235 carbon steel in 1 M HCl was 219.13 g/m^2·h at 50 ℃. When the concentration of algae extract was 200 mg/L, the corrosion rate of Q235 steel was 47.87 g/m^2·h, and the inhibition efficiency was 79.77%, which indicated that algae extract had good inhibition effect on the corrosion of Q235 steel in 1 M HCl.

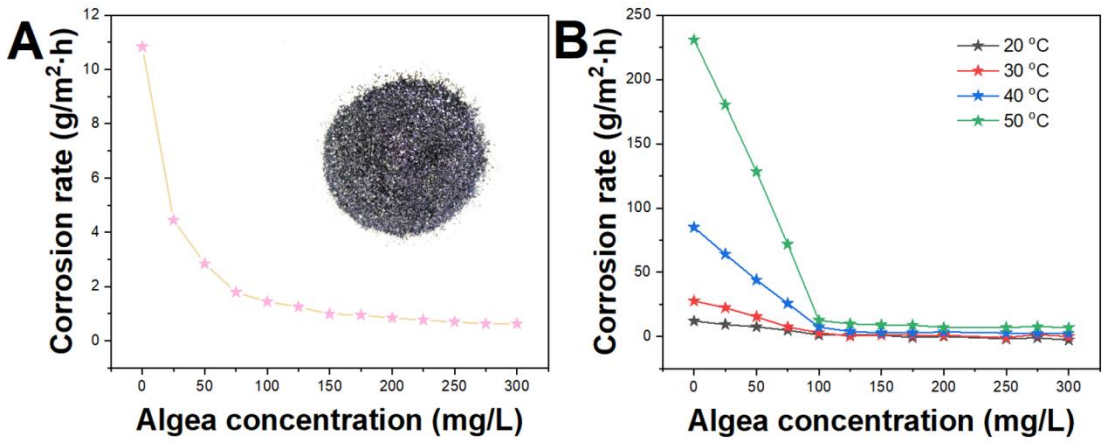

Figure 1. (A) Effects of algae extract concentration on the corrosion rate of carbon steel in 1 M HCl solution. Inset: digital photo of the algae extract by weight loss test. (B) Corrosion rate of Q235 steel in 1 M HCl at 20 ~ 50 ℃ by weight loss test.

The inhibition effect of plant inhibitors is generally due to the adsorption of organic compounds on metal surface. It is assumed that the inhibition of algae extract is produced by its adsorption on the surface of Q235 steel. When different concentrations of extracts were added, the results of weight loss experiment were fitted according to the relationship between coverage (θ) and corrosion inhibition efficiency (η%) (η% = 100 × θ). The results are shown in Figure 2 and Table 1. At different temperature, C/θ had a good linear relationship with C, and the correlation coefficient reached more than 0.999. The results showed that the adsorption of algae extract on Q235 steel surface was in accordance with Langmuir adsorption isotherm, that is, monolayer adsorption [52]. With the increase of temperature, the

adsorption coefficient K increased gradually and the adsorption capacity increased. This indicated that the adsorption process of the extract on Q235 steel surface was endothermic, and the inhibition efficiency increased accordingly.

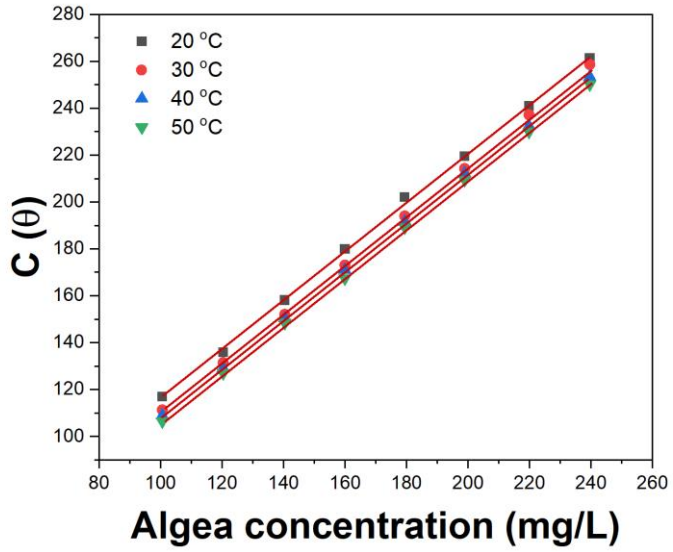

Figure 2. Adsorption isotherms of algae extract on Q235 steel in 1 M HCl at different temperature deduced from the weight loss test.

Table 1. Analysis of adsorption isotherms at different temperature.

Temperature	R	b	k	K (× 10^{-1} L/mg)	IE (%)
20	0.99997	12.03	1.045	0.961	91.9
30	0.99999	5.51	1.033	0.963	94.0
40	0.99998	2.45	1.071	0.934	95.4
50	0.99997	2.40	1.036	0.965	95.5

Figure 3 shows the self-corrosion potential time curve of Q235 steel in 1 M HCl solution with different concentrations of algae extract at 30 ℃. At the beginning of immersion, the self-corrosion potential of Q235 steel surface was very negative. With the prolongation of immersion time, the self-corrosion potential moved to the positive direction [53]. The self-corrosion potential increased obviously with the addition of inhibitor. Furthermore, with the increase of inhibitor concentration, the self-corrosion potential increased gradually. At 30 ℃, the change trend of self-corrosion potential curve of Q235 steel surface was almost the same. During the immersion process, the self-corrosion potential of Q235 steel was in a steady upward trend, and finally tended to be stable.

The self-corrosion potential of metal was related to the formation of coating film on metal surface. The relatively stable self-corrosion potential reflected that the covering film on the metal surface was completely formed [54]. That is to say, when Q235 steel was immersed in the corrosive medium,

the effective components in algae extract quickly adsorbed on the surface of Q235 steel and formed a protective film. When the adsorption reached a certain extent, the formation rate of the protective film slowed down until it reached a stable state. At that time, the self-corrosion potential tended to be stable.

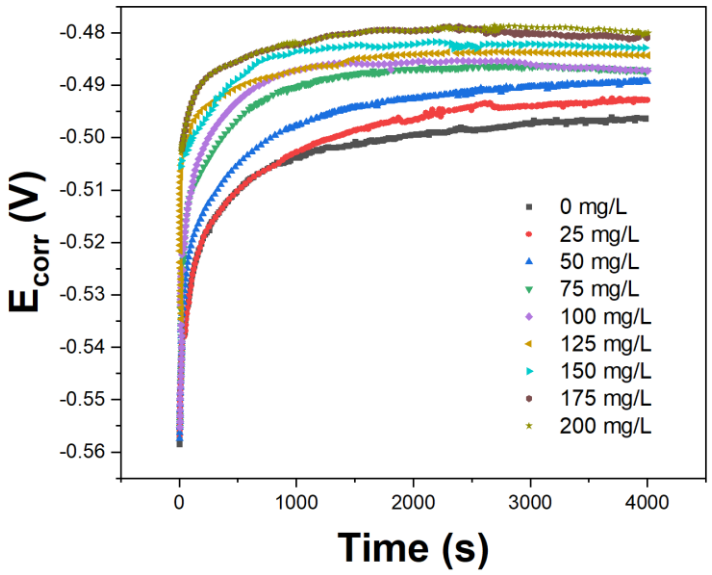

Figure 3. E_{corr} variations of Q235 steel in 1 M HCl solution with different concentrations of algae extract at 30℃.

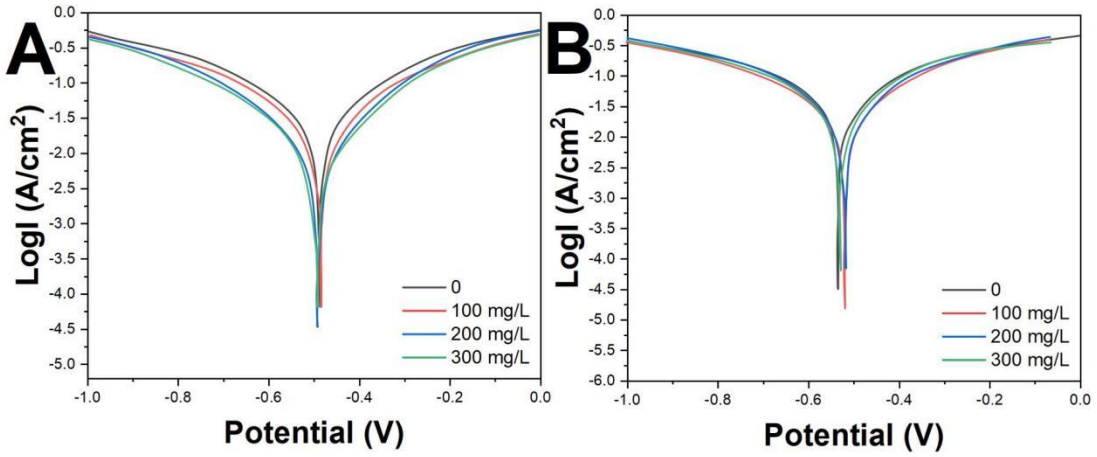

Figure 4. Potentiodynamic polarization curves of carbon steel in 1 M HCl with different concentrations of algae extract at (A) 30℃ and (B) 50℃.

Figure 4 shows the potentiodynamic polarization curve of Q235 steel in 1 M HCl with algae extract concentration of 0-300 mg/L at 30 ℃ and 50 ℃. The fitting results by Tafel linear extrapolation method are shown in Table 2. The results showed that in the range of test temperature, the shapes of cathode and anode of polarization curve changed little after adding algae extract at the same temperature

[55]. However, the polarization curves of both cathode and anode moved to the direction of I_{corr} decrease. With the increase of the concentration of the extract, I_{corr} decreased and the inhibition efficiency increased, and the change trend was the same as that measured by weight loss method. At different temperature, when the same concentration of extract was added, I_{corr} gradually increased with the increase of temperature, indicating that the corrosion was intensified [56]. The variation of I_{corr} degree was uniform with the increase of extract concentration. After adding the extract, E_{corr} changed little, while b_a and b_c increased, which indicated that the extract could inhibit the anodic process and cathodic process of carbon steel corrosion in hydrochloric acid solution.

The inhibition effect of algae extract was also compared with that of other extracts reported previously. The results are presented in Table 3, revealing that algae extract had the same anticorrosion performance as the previously reported extracts or had even better anticorrosion performance.

Table 2. Electrochemistry data of carbon steel in 1 M HCl with different concentrations of k algae extract at (A) 30℃ and (B) 50℃.

Temperature	Concentration	$-E_{corr}$ (mV)	I_{corr} (10^3 mA/cm^2)	β_a (mV/dec)	β_c (mV/dec)	η (%)
30	0	471	9.241	64	115	-
	100	458	5.860	41	113	44.59
	200	475	3.205	39	103	79.11
	300	478	2.841	41	118	82.10
50	0	475	67.44	61	118	-
	100	460	32.25	57	114	50.32
	200	458	23.54	52	117	78.60
	300	466	14.05	47	105	88.50

Table 3. Comparison of the anticorrosion performance of algae extract and other extracts.

Extract	Electrolyte	Inhibition efficiency	Reference
Locust Bean Gum	0.5 M H_2SO_4	89.8%	[57]
Papaya leaves extract	1 M HCl	81.4%	[58]
Lilium brownii leaves extract	1 M HCl	85%	[59]
Betel leaves	1 M HCl	84%	[60]
Brassica oleracea L extract	0.5 M H_2SO_4 and 1 M HCl	92.3%	[61]
Camphor leaves extract	1 M HCl	89.4%	[62]
Magnolia grandiflora	1 M HCl	85%	[63]
Algae extract	1 M HCl	88.5%	This work

The Nyquist diagram and Bode of electrochemical impedance spectroscopy (EIS) of Q235 steel in hydrochloric acid solution containing different concentrations of algae extract are shown in Figure 5.

The results showed that the arc radius of capacitive reactance in high frequency region of EIS of Q235 steel in HCl increased with the increase of extract concentration, showing a single time constant feature. The results showed that the impedance value of Q235 steel increased gradually and the corrosion resistance increased. The inductive arc in low frequency region was related to the adsorption process of corrosion inhibitor on Q235 steel surface and the unstable surface state caused by the adsorption of corrosion products containing iron on the electrode surface [64]. It can be seen from the Bode diagram that the difference of impedance modulus of Q235 steel corrosion process was small when different concentrations of extract were added. In the low frequency region, the impedance modulus increased with the increase of extract concentration,I indicating that the impedance behavior of Q235 steel in HCl was closer to pure capacitance. The peak value of phase angle increased with the increase of extract concentration, which indicated that the corrosion resistance of Q235 steel in hydrochloric acid solution increased gradually. In the low frequency region, a phase angle curve less than 0 ° appeared, which indicated that there may be an equilibrium process of adsorption and desorption of corrosion inhibitor and corrosion products on Q235 steel surface [65,66].

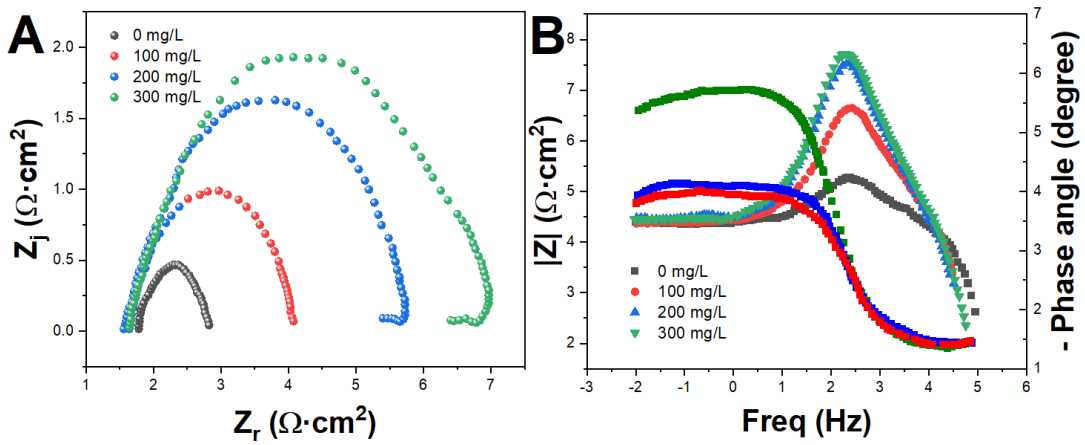

Figure 5. (A) Nyquist plots and (B) Bode plots of Q235 steel in 1 M HCl solution with different concentration of algae extract at 30℃

The results in Table 3 show that the charge transfer resistance R_t increased gradually with the increase of the concentration of the extract. The charge transfer process of the corrosion reaction of carbon steel in hydrochloric acid solution was blocked, and the corrosion resistance of carbon steel was enhanced. The parameter n with different concentrations of extract was close to 1, indicating that it tended to be pure capacitance. Y_0 value decreased slightly with the increase of the extract concentration, indicating that the extract was adsorbed on the surface of carbon steel.

Table 3. Impedance data of Q235 steel in 1 M HCl solution with different concentrations of algae extract at 30°C

Extract (mg/L)	R_s ($\Omega \cdot cm^2$)	Y_0 ($F \cdot cm^2$)	n	R_t ($\Omega \cdot cm^2$)
0	3.748	1.7×10^{-3}	0.84	1.488
100	1.591	1.6×10^{-3}	0.81	2.409
200	1.491	1.4×10^{-3}	0.81	4.287
300	1.657	1.1×10^{-3}	0.81	5.520

Figure 6 shows the infrared spectrum of algae extract powder samples. There was a strong absorption peak at 3425.11 cm^{-1}, which was the superposition of carboxyl –COOH stretching vibration and O-H stretching vibration. The absorption peak near 2924.22 cm^{-1} was methylene $–CH_2$ asymmetric stretching vibration [67]. 2854.61 cm^{-1} was the stretching vibration of C–H [68]. There was C=O stretching vibration near 1626.17 cm^{-1}, 1538.91 cm^{-1} and 1415.22 cm^{-1} were the stretching vibration of C=C. 1379.60 cm^{-1} was the in-plane bending vibration of C–H. 1264.36 cm^{-1} and 1116.90 cm^{-1} were the skeleton vibrations of symmetrical ring and benzene ring of epoxy group [69,70]. 1073.96 cm^{-1} was the antisymmetric stretching vibration of C–O–C. 1048.77 cm^{-1} was C–N stretching vibration. Figure 6 also indicates the transmission spectrum of the surface adsorbate of Q235 steel after being soaked in HCl ith 200 mg/L algea extract for 1 hour. The superposition of O–H stretching vibration and N–H stretching vibration moved from 3411.28 cm^{-1} to 3448.15 cm^{-1} [71]. The asymmetric stretching vibration peak of methylene – CH_2 shifted from 2924.11 cm^{-1} to 2922.85 cm^{-1}.

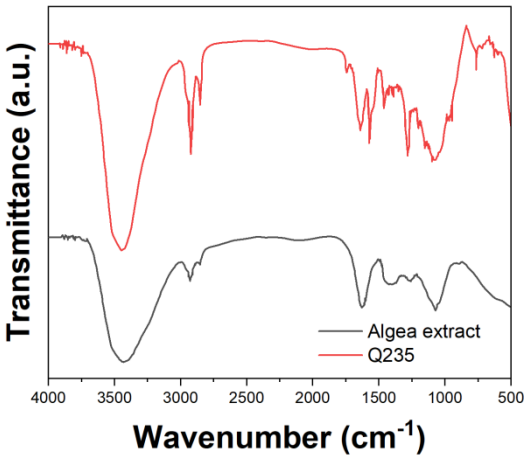

Figure 6. FTIR spectra of algae extract and surface film of the Q235 steel after being immersed in 1 M HCl containing 200 mg/L algae extract for 1 hour.

The stretching vibration of C–H moved from 2854.61 cm^{-1} to 2852.29 cm^{-1} [72]. The C=O stretching vibration peak moved from 1626.17 cm^{-1} to 1637.38 cm^{-1}. The stretching vibration of C=C moved from 1538.91 cm^{-1} and 1417.18 cm^{-1} to 1566.13 cm^{-1} and 1462.27 cm^{-1}, respectively. The in-plane bending vibration of C–H moved from 1379.60 cm^{-1} to 1395.13 cm^{-1} [73]. The skeleton vibration

of symmetrical ring and benzene ring of epoxy group moved from 1264.36 cm^{-1} and 1116.90 cm^{-1} to 1280.15 cm^{-1} and 1146.29 cm^{-1}, respectively. The antisymmetric stretching vibration of C–O–C moves from 1073.96 cm^{-1} to 1087.40 cm^{-1}. The C–H bending vibration of benzene ring moved from 894.71 cm^{-1} to 761.29 cm^{-1}. The =CH out of plane bending vibration of benzene ring moved from 601.55 cm^{-1} to 599.70 cm^{-1} [74]. It can be inferred that the extract contained oxygen and nitrogen functional groups (–COOH, O–H, C=O, N–H, C–N, C–O). In addition, algae extract contained epoxy group and benzene ring with general corrosion inhibitor structure, making it easy to bond with Q235 steel and having good corrosion inhibition effect on Q235 steel.

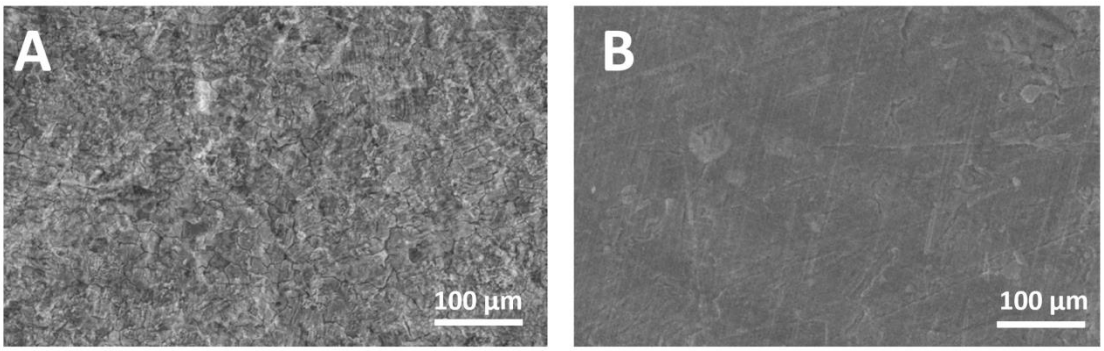

Figure 7. SEM images of Q235 steel surface after immersion for 2 hours in 1 M HCl (A) without algae extract and (B) with 200 mg/L algae extract.

Figure 7 is the SEM picture of Q235 steel surface after 2-hour reaction in HCl with and without 200 mg/L algae extract. It can be seen from the figure that the corrosion of Q235 steel in HCl was serious without adding algae extract. After adding algae extract, there was no obvious corrosion trace on the surface of Q235 steel, which indicated that algae extract was adsorbed on the surface of Q235 steel and enhanced its corrosion resistance in HCl.

4. CONCLUSION

Algae leaf extract, as a mixed inhibitor, has a remarkable effect of inhibition on Q235 steel in HCl. The inhibition efficiency can reach 80% when the dosage is 200 mg/L. With the increase of inhibitor concentration and temperature, the efficiency of inhibition increases gradually. The adsorption of inhibitor molecules on Q235 steel surface is physical in nature based on the Langmuir monolayer adsorption model. Algae extract contains oxygen atoms, nitrogen atoms and other functional groups (–COOH, O–H, C=O, N–H, C–N, C–O). In addition, the epoxy group and benzene ring contained in the algae extract have a general corrosion inhibitor structure. These effective components form a dense and uniform protective film on the surface of Q235 steel, which effectively inhibits Q235 steel from acid corrosion.

ACKNOWLEDGEMENT
This work was financially supported by Fujian Provincial Education Department Project - Young and Middle-aged Teacher Education Research Project (JAT190460), Fujian Provincial Natural Science Foundation - University Joint Fund Project (2020J01939) and Fujian Provincial Science and Technology Plan Project - University Cooperation Project (2019H6025).

References

1. A. Singh, K. Ansari, D.S. Chauhan, M. Quraishi, H. Lgaz, I.-M. Chung, *J. Colloid Interface Sci.*, 560 (2020) 225–236.
2. Q. Wang, B. Tan, H. Bao, Y. Xie, Y. Mou, P. Li, D. Chen, Y. Shi, X. Li, W. Yang, *Bioelectrochemistry*, 128 (2019) 49–55.
3. D.S. Chauhan, A.M. Kumar, M. Quraishi, *Chem. Eng. Res. Des.*, 150 (2019) 99–115.
4. B. Tan, B. Xiang, S. Zhang, Y. Qiang, L. Xu, S. Chen, J. He, *J. Colloid Interface Sci.*, 582 (2020) 918–931.
5. A. Dehghani, G. Bahlakeh, B. Ramezanzadeh, M. Ramezanzadeh, *J. Mol. Liq.*, 277 (2019) 895–911.
6. J.V. Nardeli, C.S. Fugivara, M. Taryba, E.R. Pinto, M. Montemor, A.V. Benedetti, *Prog. Org. Coat.*, 135 (2019) 368–381.
7. R.G.M. de Araújo Macedo, N. do Nascimento Marques, J. Tonholo, R. de Carvalho Balaban, *Carbohydr. Polym.*, 205 (2019) 371–376.
8. Y. Ye, D. Yang, H. Chen, *J. Mater. Sci. Technol.*, 35 (2019) 2243–2253.
9. D.S. Chauhan, K.E. Mouaden, M. Quraishi, L. Bazzi, *Int. J. Biol. Macromol.*, 152 (2020) 234–241.
10. K. Ansari, D.S. Chauhan, M. Quraishi, M.A. Mazumder, A. Singh, *Int. J. Biol. Macromol.*, 144 (2020) 305–315.
11. H. Li, S. Zhang, B. Tan, Y. Qiang, W. Li, S. Chen, L. Guo, *J. Mol. Liq.*, 305 (2020) 112789.
12. C.M. Fernandes, T. da S.F. Fagundes, N.E. dos Santos, T.S. de M. Rocha, R. Garrett, R.M. Borges, G. Muricy, A.L. Valverde, E.A. Ponzio, *Electrochimica Acta*, 312 (2019) 137–148.
13. L. Guo, R. Zhang, B. Tan, W. Li, H. Liu, S. Wu, *J. Mol. Liq.*, 310 (2020) 113239.
14. E. Alibakhshi, M. Ramezanzadeh, S. Haddadi, G. Bahlakeh, B. Ramezanzadeh, M. Mahdavian, *J. Clean. Prod.*, 210 (2019) 660–672.
15. R. Farahati, A. Ghaffarinejad, S.M. Mousavi-Khoshdel, J. Rezania, H. Behzadi, A. Shockravi, *Prog. Org. Coat.*, 132 (2019) 417–428.
16. Z. Sanaei, M. Ramezanzadeh, G. Bahlakeh, B. Ramezanzadeh, *J. Ind. Eng. Chem.*, 69 (2019) 18–31.
17. H. Karimi-Maleh, B.G. Kumar, S. Rajendran, J. Qin, S. Vadivel, D. Durgalakshmi, F. Gracia, M. Soto-Moscoso, Y. Orooji, F. Karimi, *J. Mol. Liq.*, 314 (2020) 113588.
18. Q. Liu, Y. Zheng, L. Fu, B.A. Simco, C.A. Goudie, *Aquaculture*, 532 (2021) 735952.
19. L. Fu, W. Su, F. Chen, S. Zhao, H. Zhang, H. Karimi-Maleh, A. Yu, J. Yu, C.-T. Lin, *Bioelectrochemistry* (2021) 107829.
20. L. Fu, Y. Zheng, P. Zhang, H. Zhang, M. Wu, H. Zhang, A. Wang, W. Su, F. Chen, J. Yu, W. Cai, C.-T. Lin, *Bioelectrochemistry*, 129 (2019) 199–205.
21. Y. Xu, Y. Lu, P. Zhang, Y. Wang, Y. Zheng, L. Fu, H. Zhang, C.-T. Lin, A. Yu, *Bioelectrochemistry*, 133 (2020) 107455.
22. E. Ebenso, N. Eddy, A. Odiongenyi, *Afr. J. Pure Appl. Chem.*, 2 (2008) 107–115.
23. R.A.L. Sathiyanathan, M.M. Essa, S. Maruthamuthu, M. Selvanayagam, N. Palaniswamy, *J. Indian Chem. Soc.*, 82 (2005) 357–359.
24. K. Parikh, K. Joshi, *Trans.-Soc. Adv. Electrochem. Sci. Technol.*, 39 (2004) 29.
25. A. Iranbakhsh, M. Ebadi, M. Bayat, *Glob. Vet.*, 4 (2010) 149–155.

26. E. Mansour, A. Abdel-Gaber, B. Abd-El Nabey, N. Khalil, E. Khamis, A. Tadros, H. Aglan, A. Ludwick, *Corrosion*, 59 (2003) 242–249.
27. H. Karimi-Maleh, Y. Orooji, F. Karimi, M. Alizadeh, M. Baghayeri, J. Rouhi, S. Tajik, H. Beitollahi, S. Agarwal, V.K. Gupta, *Biosens. Bioelectron.* (2021) 113252.
28. H. Karimi-Maleh, M. Alizadeh, Y. Orooji, F. Karimi, M. Baghayeri, J. Rouhi, S. Tajik, H. Beitollahi, S. Agarwal, V.K. Gupta, S. Rajendran, S. Rostamnia, L. Fu, F. Saberi-Movahed, S. Malekmohammadi, *Ind. Eng. Chem. Res.*, 60 (2021) 816–823.
29. H. Karimi-Maleh, A. Ayati, R. Davoodi, B. Tanhaei, F. Karimi, S. Malekmohammadi, Y. Orooji, L. Fu, M. Sillanpää, *J. Clean. Prod.*, 291 (2021) 125880.
30. L. Fu, K. Xie, A. Wang, F. Lyu, J. Ge, L. Zhang, H. Zhang, W. Su, Y.-L. Hou, C. Zhou, C. Wang, S. Ruan, *Anal. Chim. Acta*, 1081 (2019) 51–58.
31. J. Zhou, Y. Zheng, J. Zhang, H. Karimi-Maleh, Y. Xu, Q. Zhou, L. Fu, W. Wu, *Anal. Lett.*, 53 (2020) 2517–2528.
32. G.G. de Souza, M.T. de Sampaio, A.B. Furtado, P.H. Buzzetti, R.N. Damasceno, E.A. Ponzio, C.J. Ramos, V.L. Teixeira, J.A. Velasco, *Rev. Virtual Quimica*, 11 (2019) 1521–1539.
33. T. Benabbouha, R. Nmila, M. Siniti, K. Chefira, H. El Attari, H. Rchid, *SN Appl. Sci.*, 2 (2020) 1–11.
34. A. Dehghani, G. Bahlakeh, B. Ramezanzadeh, *J. Mol. Liq.*, 282 (2019) 366–384.
35. M.P. Asfia, M. Rezaei, G. Bahlakeh, *J. Mol. Liq.*, 315 (2020) 113679.
36. A. Dehghani, G. Bahlakeh, B. Ramezanzadeh, M. Ramezanzadeh, *J. Mol. Liq.*, 277 (2019) 895–911.
37. L. Fu, Y. Zheng, P. Zhang, H. Zhang, W. Zhuang, H. Zhang, A. Wang, W. Su, J. Yu, C.-T. Lin, *Biosens. Bioelectron.*, 120 (2018) 102–107.
38. M. Zhang, B. Pan, Y. Wang, X. Du, L. Fu, Y. Zheng, F. Chen, W. Wu, Q. Zhou, S. Ding, *ChemistrySelect*, 5 (2020) 5035–5040.
39. W. Long, Y. Xie, H. Shi, J. Ying, J. Yang, Y. Huang, H. Zhang, L. Fu, *Fuller. Nanotub. Carbon Nanostructures*, 26 (2018) 856–862.
40. Y. Zheng, Y. Huang, H. Shi, L. Fu, *Inorg. Nano-Met. Chem.*, 49 (2019) 277–282.
41. Y. Zheng, H. Zhang, L. Fu, *Inorg. Nano-Met. Chem.*, 48 (2018) 449–453.
42. G. Liu, X. Yang, H. Zhang, L. Fu, *Int J Electrochem Sci*, 15 (2020) 5395–5403.
43. W. Wu, Q. Zhou, Y. Zheng, L. Fu, J. Zhu, H. Karimi-Maleh, *Int J Electrochem Sci*, 15 (2020) 10093–10103.
44. L. Fu, Z. Liu, J. Ge, M. Guo, H. Zhang, F. Chen, W. Su, A. Yu, *J. Electroanal. Chem.*, 841 (2019) 142–147.
45. R. Yang, B. Fan, S. Wang, L. Li, Y. Li, S. Li, Y. Zheng, L. Fu, C.-T. Lin, *Micromachines*, 11 (2020) 967.
46. J. Ying, Y. Zheng, H. Zhang, L. Fu, *Rev. Mex. Ing. Quím.*, 19 (2020) 585–592.
47. X. Zhang, R. Yang, Z. Li, M. Zhang, Q. Wang, Y. Xu, L. Fu, J. Du, Y. Zheng, J. Zhu, *Rev. Mex. Ing. Quím.*, 19 (2020) 281–291.
48. W. Wu, M. Wu, J. Zhou, Y. Xu, Z. Li, Y. Yao, L. Fu, *Sens. Mater.*, 32 (2020) 2941–2948.
49. L. Fu, A. Wang, G. Lai, W. Su, F. Malherbe, J. Yu, C.-T. Lin, A. Yu, *Talanta*, 180 (2018) 248–253.
50. S.A. Haddadi, E. Alibakhshi, G. Bahlakeh, B. Ramezanzadeh, M. Mahdavian, *J. Mol. Liq.*, 284 (2019) 682–699.
51. A. Dehghani, G. Bahlakeh, B. Ramezanzadeh, *J. Mol. Liq.*, 282 (2019) 366–384.
52. M.P. Asfia, M. Rezaei, G. Bahlakeh, *J. Mol. Liq.*, 315 (2020) 113679.
53. I.B. Onyeachu, I.B. Obot, A.A. Sorour, M.I. Abdul-Rashid, *Corros. Sci.*, 150 (2019) 183–193.
54. A. Dehghani, G. Bahlakeh, B. Ramezanzadeh, M. Ramezanzadeh, *J. Mol. Liq.*, 277 (2019) 895–911.
55. J.D. Olivo, B. Brown, D. Young, S. Nešić, *Corrosion*, 75 (2019) 137–139.

56. M. Izadi, T. Shahrabi, I. Mohammadi, B. Ramezanzadeh, A. Fateh, *Compos. Part B Eng.*, 171 (2019) 96–110.
57. L. Guo, R. Zhang, B. Tan, W. Li, H. Liu, S. Wu, *J. Mol. Liq.*, 310 (2020) 113239.
58. B. Tan, B. Xiang, S. Zhang, Y. Qiang, L. Xu, S. Chen, J. He, *J. Colloid Interface Sci.*, 582 (2021) 918–931.
59. X. Zuo, W. Li, W. Luo, X. Zhang, Y. Qiang, J. Zhang, H. Li, B. Tan, *J. Mol. Liq.*, 321 (2021) 114914.
60. B. Tan, J. He, S. Zhang, C. Xu, S. Chen, H. Liu, W. Li, *J. Colloid Interface Sci.*, 585 (2021) 287–301.
61. H. Li, Y. Qiang, W. Zhao, S. Zhang, *Colloids Surf. Physicochem. Eng. Asp.*, 616 (2021) 126077.
62. S. Chen, H. Zhao, S. Chen, P. Wen, H. Wang, W. Li, *J. Mol. Liq.*, 312 (2020) 113433.
63. S. Chen, S. Chen, B. Zhu, C. Huang, W. Li, *J. Mol. Liq.*, 311 (2020) 113312.
64. A.A. Farag, M. Migahed, E. Badr, *J. Bio- Tribo-Corros.*, 5 (2019) 1–12.
65. C. Li, Y. Ma, *Int J Electrochem Sci*, 15 (2020) 1964–1981.
66. S. Udensi, O. Ekpe, L. Nnanna, *Chem. Afr.*, 3 (2020) 303–316.
67. Y. Ye, D. Yang, H. Chen, *J. Mater. Sci. Technol.*, 35 (2019) 2243–2253.
68. P.S. Neriyana, V.D. Alva, *Chem. Afr.*, 3 (2020) 1087–1098.
69. L. Fockaert, T. Würger, R. Unbehau, B. Boelen, R.H. Meißner, S.V. Lamaka, M.L. Zheludkevich, H. Terryn, J. Mol, *Electrochimica Acta*, 345 (2020) 136166.
70. S. Sharma, Y. Sharma, *Port. Electrochimica Acta*, 37 (2019) 1–22.
71. N. Baig, D. Chauhan, T.A. Saleh, M. Quraishi, *New J. Chem.*, 43 (2019) 2328–2337.
72. G. Palumbo, K. Berent, E. Proniewicz, J. Banaś, *Materials*, 12 (2019) 2620.
73. Z. Zhang, H. Ba, Z. Wu, *Constr. Build. Mater.*, 227 (2019) 117080.
74. S.A. Akintola, M. Oki, A. Aleem, A. Adediran, O. Akpor, O.M. Oluba, B. Ogunsemi, P. Ikubanni, *Results Eng.*, 4 (2019) 100026.